JOURNAL OF PROPULSION AND POWER
Vol. 21, No. 4, July–August 2005

Design Optimization of Rocket-Based Combined-Cycle Inlet/Ejector System

M. Nayem Jahingir* and Ziaul Huque†
Prairie View A&M University, Prairie View, Texas 77446

The results of optimizing some of the geometric design variables of the inlet/ejector section of a rocket-based combined-cycle (RBCC) engine and the study of its performance trends are presented. A two-dimensional rocket-ejector system was studied over a matrix of engine design variables. Bypass ratio, ejector compression ratio, and ejector/mixer thrust efficiency were used to analyze RBCC internal flowpath physics. The primary thruster exit flow properties were calculated with the reacting and multiphase program, which was used as fixed inlet conditions for the ejector/mixer analysis. The computational fluid dynamics simulations of the inlet/ejector system were carried out with a finite difference Navier–Stokes code. The GO_2/GH_2 combustion physics were solved for finite rate conditions with a system of seven species and nine reactions. Neural networks techniques were used to generate the response surface. The desirability function approach of optimization, tied with the response surface, was used for inlet/ejector optimization. This approach gives the designers the freedom to set up their own priorities on the response values to be built into the optimization procedure. Optimum values of primary thruster size, duct length-to-diameter ratio and ramjet burner to ejector/mixer inlet area ratio were obtained. Engine performance trends as functions of geometric variables were also studied.

Nomenclature

A_s/A_p	=	secondary to primary flow area ratio
A_8/A_5	=	ramjet burner to ejector/mixer inlet area ratio
D	=	desirability function
L/D	=	ejector/mixer aspect ratio
β	=	bypass ratio
η_t	=	ejector/mixer thrust (nozzle) efficiency

Introduction

A MAJOR goal driving current space propulsion research is to decrease significantly the cost of access to space. There are currently efforts underway to develop reusable launch vehicles that promise to decrease long-term costs as compared to the traditional expendable staged vehicles. One way to use high-efficiency air-breathing cycles during ascent in a reusable system is through the use of combined-cycle propulsion (CCP) systems. CCP systems can be broadly divided into two categories: airbreathing combined cycles and combined-cycle systems that include a rocket subsystem. Airbreathing combined-cycle engines are intended primarily for missions involving high-speed cruise in the atmosphere, but are not candidates for transatmospheric flight. Out of many types and variations of CCP systems, one class of rocket-based CCP systems shows promise for Earth-to-orbit (ETO) missions. These are engines that operate in rocket-ejector mode and also have the capability of operating in ramjet, scramjet, and rocket-only modes and are typically referred to as rocket-based combined-cycle (RBCC) engines. A schematic of an RBCC engine is shown in Fig. 1. Many of the advantages of RBCC engines result from certain synergistic benefits that would not occur if the two units operated separately.[1] The ability to use the rocket as an ejector increases the thrust. Afterburning in rocket-ejector mode, using the ramjet/scramjet fuel injectors, further increases the thrust and specific impulse compared to the rocket alone. The specific impulse continues to increase with the increasing flight speed because the cycle more closely resembles ramjet operation. In ramjet and scramjet modes, the rocket could be advantageously used as a fuel injector and mixing enhancer. In the rocket-only mode, the use of the engine duct as a highly expanded nozzle at high altitudes increases the specific impulse of that mode of operation. Another key advantage of RBCC systems is the reduction in the amount of onboard oxidizer required. This decreases the size and, therefore, the weight, of the tank and vehicle.[2]

An integrated inlet/ejector is one of the most critical parts of an RBCC engine propulsion system. Its design must be such that it delivers air to the engine at the desired mass flow rate and flow conditions for all flight Mach numbers. This delivery must be accompanied by as few losses, drag, weight, and complexity as possible. In short, the design is a tradeoff or compromise between a high-pressure recovery and low drag. This compromise can only be found after several propulsion and vehicle performance calculations, which strongly depend on the mission of the vehicle.

The objective of this paper is to optimize the inlet/ejector system of an RBCC engine. For this purpose, a two-dimensional rocket-ejector system was studied over a matrix of engine design variables. Figure 1 defines some of the RBCC engine design variables. Each variable had three values, so that the initial trade space was 27 configurations as shown in Table 1. A 28th configuration was run to explore the effect of a constant-area mixer ($A_8/A_5 = 1.0$). The performance of the ejector/mixer was measured with the following figures of merit (FOM): bypass ratio, ratio of secondary flow to primary flow, ejector compression ratio (ECR), ratio of total pressure at the ejector/mixer exit to total pressure of secondary flow and ejector/mixer thrust (nozzle) efficiency, and thrust at the exit divided by thrust at the mixer inlet. Primary thruster mass flow rates were kept constant for all configurations, but each A_s/A_p ratio resulted in a different primary thruster area ratio and, therefore, a different primary thruster exit pressure. The primary thruster exit flow properties were calculated with the reacting and multiphase program.

Approaches

Computational Fluid Dynamic (CFD) Simulation

The RBCC flowpath configuration for this analysis was two dimensional with a single primary thruster on the engine centerline.

Presented as Paper 2003-5232 at the AIAA/ASME/SAE/ASEE 39th Joint Propulsion Conference and Exhibit, Huntsville, AL, 20–23 July 2003; received 10 May 2004; revision received 29 December 2004; accepted for publication 3 January 2004.

*Research Assistant, Computational Fluid Dynamics Institute, Department of Mechanical Engineering; currently Research Engineer, ANATECH Corporation, 5435 Oberlin Drive, San Diego, CA 92126. Member AIAA.

†Associate Professor, Computational Fluid Dynamics Institute, Department of Mechanical Engineering.

Table 1 RBCC inlet/ejector design trade space

Design variables	$L/D=7$			$L/D=14$			$L/D=21$		
	$As/Ap=4.5$	$As/Ap=7.3$	$As/Ap=15.6$	$As/Ap=4.5$	$As/Ap=7.3$	$As/Ap=15.6$	$As/Ap=4.5$	$As/Ap=7.3$	$As/Ap=15.6$
$A8/A5=1.0$									×
$A8/A5=1.5$	×	×	×	×	×	×	×	×	×
$A8/A5=2.0$	×	×	×	×	×	×	×	×	×
$A8/A5=2.5$	×	×	×	×	×	×	×	×	×

Table 2 Primary thruster exit conditions for different design configuration

Design variables A_s/A_p	Chamber pressure P_i, atm	Exit pressure P_e, atm	Pressure ratio P_i/P_e	Supersonic area ratio A_e/A_t	Velocity at rocket exit, m/s	Temperature at rocket exit, K
4.55	34.08	0.7	48.625	9	1289.7	1604.65
7.33	34.08	1.04	32.730	6	1338.0	1737.94
15.66	34.08	2.08	16.365	3	1422.7	1988.1

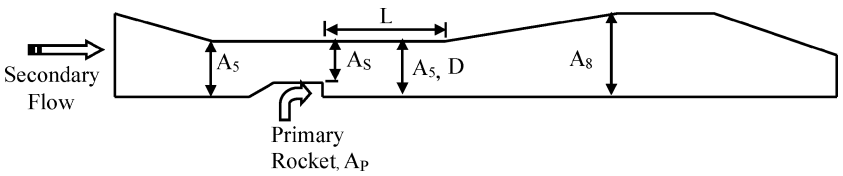

Fig. 1 Schematic of two-dimensional axisymmetric RBCC engine.

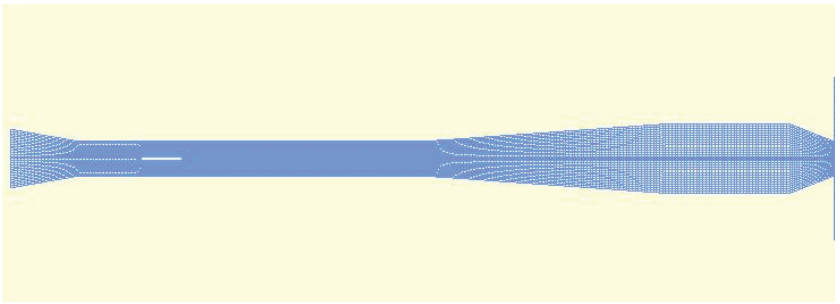

Fig. 2 Grid distribution for $L/D=14$, $A_s/A_p=7.33$, and $A_8/A_5=2.0$ RBCC engine configuration (excluding far-field boundaries).

The primary thruster was housed in a centerbody that created an annular constant area inlet. The inlet/ejector plane is defined to be the exit plane of the primary thruster. The secondary inlet length L was a function of two of the trade space variables, L/D and A_s/A_p. A_s is the area of the secondary flow at the mixer inlet plane, and A_p is the area of the primary thruster exit plus any base area surrounding the thruster. A_5 is the total flow area at the ejector/mixer inlet plane ($A_s + A_p$), and A_8 is the flow area of the ramjet burner. The computational fluid dynamics (CFD) simulation of the RBCC internal flowpath was performed with a finite difference Navier–Stokes (FDNS) code.[3,4] The code solves the Reynolds-averaged transport equations with a variety of options for physical models and boundary conditions. A pressure-based predictor plus multiple corrector solution method is employed so that flow over a wide speed range (from low subsonic to supersonic) can be analyzed. The present analysis was solved steady state, implementing the third-order total variation diminishing scheme and an extended two-equation turbulence model with compressibility correction. The GO_2/GH_2 combustion physics are solved as a system of seven species and nine reactions.[5,6]

Grid Description

To obtain a grid-independent solution, several grid density parametrics were performed. The computational domain consists of a two-dimensional representation of the experimental hardware internal flowpath and is shown in Fig. 2. The structured grid had approximately 15,000 nodes in 15 zones. Nonmatching zonal boundaries were implemented at several locations to keep the number of nodes from becoming excessive. The geometric definition of the 27 configurations was provided by an engine design spreadsheet. All grids contained the same number of nodes in the freestream, inlet, ram burner, and nozzle portions of the domain. The number of nodes in the axial direction of the ejector/mixer varied because of their different lengths. A consistent axial delta-s was used in the ejector/mixer region. The blockage created by the rocket engine was modeled in the flowpath; however, the rocket engine's internal flowpath was not contained in the present computational domain.

Boundary Conditions

The geometry of an RBCC engine to be analyzed has two inlet boundaries. One is for the secondary air inlet and the other one is for the primary thruster inlet. In real practice, the primary thruster was built as an integral part of the RBCC engine system, but for computational benefit the rocket engine's flow computation was performed separately.

Primary Thruster Simulation

A one-dimensional rocket simulator code for the calculation of complex chemical equilibrium compositions and applications (CEA)[7] was used to calculate the rocket exit properties for different primary thruster area ratios. For this analysis, primary thruster size was varied to justify the amount of secondary air entrainment. This GO_2/GH_2 primary rocket was designed to operate at an operation pressure of 3.45 MPa with oxygen to fuel (O/F) ratio of 4.0. The three different A_s/A_p ratios resulted in three different supersonic area ratios, which drastically change the rocket outlet conditions. Table 2 summarizes the results of individual rocket analysis with a chemical equilibrium code for three different design conditions.

These thruster exit flow properties were defined as fixed inlet conditions for the ejector/mixer analysis.

Inflow, Outflow, and Engine Surface Boundaries

In the computational model, the secondary inlet was specified as a subsonic, fixed total condition boundary. In this boundary, the values of two dependent flowfield variables were stipulated, whereas the values of other variables were allowed to float. The rocket nozzle exit condition was supersonic and was used as a fixed inlet condition for the RBCC engine analysis. All engine surfaces were set to no-slip adiabatic walls, and the centerline of the engine was set to a symmetric boundary condition. The zones downstream of the nozzle had a far-field boundary condition applied that maintained one atmosphere pressure on the boundary. The rightmost face was set as an exit boundary.

Combustion Modeling

The GO_2/GH_2 combustion physics were solved for finite rate with a system of seven species and nine reactions using FDNS. In this analysis, it was assumed that the excess GH_2 in the rocket plume depleted the GO_2 in the airstream and that there was no downstream introduction of GH_2.

Neural Network

Neural networks are composed of simple elements operating in parallel. As in nature, the network function is determined largely by the connections between elements.[8] A neural network (NN) can be trained to perform a particular function by adjustment of the values of the connections (weights) between elements. Commonly, NNs are adjusted, or trained, so that a particular input leads to a specific target output. The network is adjusted, based on a comparison of the output and the target, until the network output matches the target. Typically, many such input/target pairs are used in this supervised learning to train a network. In this study, a backpropagation NN was used. Standard backpropagation is a gradient descent algorithm. The term backpropagation refers to the manner in which the gradient is computed for nonlinear multilayer networks. The present study used an NN to build a response surface from 27 CFD runs of a steady-state flow of an inlet/ejector system, and it was later used for evaluating an objective function. The data were entered into the net as a $[3 \times 1]$ matrix. In the first layer, a "tansig" function from the MATLAB® NN toolbox was used as a transfer function in three neurons. Tansig is a short name for hyperbolic tangent sigmoid function. Tansig (N) takes one input N, which is a matrix of net input (column) vectors, and returns each element of N squashed between -1 and 1. In the second layer, a "purelin" function was used in one neuron. Purlin is a transfer function that calculates a layer's output from its net input.

Optimization Approach

In this paper, the desirability approach of optimization, tied with response surface and an NN technique, has been used for response surface generation and inlet/ejector optimization. The desirability function approach is one of the most widely used methods in industry for the optimization of multiple-response processes. The method allows the designer's own priorities on the response values to be built into the optimization procedure. One method of optimizing multiple responses simultaneously is to build a composite response known as the desirability function from the individual responses. It is based on the idea that the quality of a product or process that has multiple quality characteristics, with one of them outside of some desired limits, is completely unacceptable. The method finds operating conditions that provide the most desirable response values. The method gives designers the freedom to set up their own priorities on the response values to be built into the optimization procedure. The desirability approach of optimization was successfully used in the rocket engine ejector optimization.[9]

In the current study, it is desirable to maximize simultaneously the bypass ratio β, ECR, and ejector/mixer thrust (nozzle) efficiency η_t. The first step is to develop a desirability function D for each response. In the case where a response should be maximized, such as β, the desirability takes the form

$$D_1 = [(\beta - A)/(C - A)]^S$$

where C is the target value and A is the lowest acceptable value such that $D_1 = 1.0$ for any $\beta > C$ and $D_1 = 0$ for $\beta < A$. For bypass ratio, a target value of 4.5 and a minimum value of 0.5 were assumed.

In the case of maximizing ECR, the desirability takes the form

$$D_2 = [(\mathrm{ECR} - F)/(E - F)]^t$$

where E is the target value and F is the lowest acceptable value such that $D_2 = 1.0$ for any ECR $> E$ and $D_2 = 0$ for ECR $< F$. For ECR, a target value of 2.0 and a minimum value of 1.0 were assumed.

To maximize ejector/mixer thrust (nozzle) efficiency η_t, the desirability function takes the form

$$D_3 = [(\eta_t - G)/(H - G)]^u$$

where H is the target value and G is the lowest acceptable value such that $D_3 = 1.0$ for any $\eta_t > H$ and $D_3 = 0$ for $\eta_t < G$. For ejector/mixer thrust efficiency, a target value of 1.0 and a minimum value of 0.1 were assumed.

The power values s, t, and u in the expressions of the aforementioned desirability functions are weighting factors and are set to 1.0 assuming linear desirability functions. Choices for A, C, E, F, G, and H are chosen according to the designer's priorities or, as in the present study, simply as the boundary values of the domain of β, ECR, and η_t.

A single-composite response is developed that is the geometric mean of the desirabilities of individual responses. The composite response is defined as

$$D = (D_1 \times D_2 \times D_3, \ldots, D_m)^{1/m}$$

which, for the present case, is

$$\text{minimized} \quad D = (1/D_1 \times 1/D_2 \times 1/D_3)^{\frac{1}{3}}$$

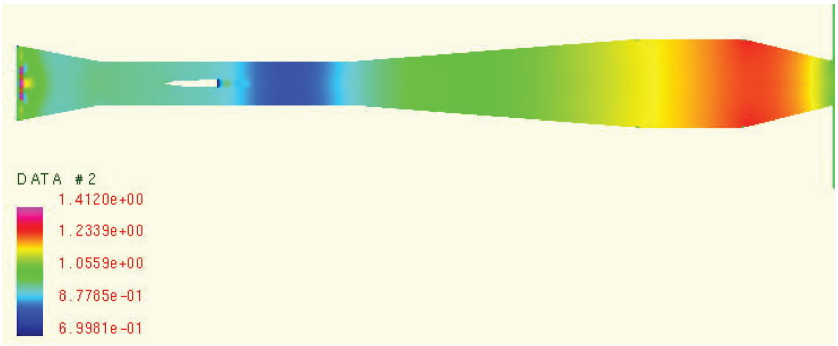

Fig. 3 Static pressure contour of RBCC engine internal flowpath for configuration $L/D = 7$, $A_s/A_p = 4.55$, and $A_8/A_5 = 2.0$ (case 2).

The reciprocal of each individual response was considered as the total desirability, which is subject to minimization. This is then submitted to a nonlinear gradient-based optimizer NPSOL,[10] to be minimized. In this analysis, there were three design variables; X_1, which represents the isolator aspect ratio L/D; X_2, which represents secondary to primary area ratio A_s/A_p; and X_3, which represents ram burner to total mixture area ratio A_8/A_5.

The CFD data of 27 cases were used to generate a response surface. This response surface was used for training the NN, and later it was used for objective function evaluation during the optimization process. The optimization was done for a simple bounded form, in which the objective function is both subject to the domain variables and linear constraints. Some of the RBCC optimal constraints are mentioned in Ref. 11, but the applied constraint was chosen arbitrarily to show the effect of constraints existence. Boundary values of the variables were set as $7 < X_1 < 21$, $4 < X_2 < 16$, and $1 < X_3 < 3$, and the relationship between the isolator aspect ratio L/D and the ram burner and mixture inlet area ratio A_8/A_5 was considered as a linear constraint. That is, $X_1 - 4X_3 > 0.0$

Table 3 Summary of FOM

Design variables	Bypass ratio	Ejector compression ratio	Mixer thrust coefficient
Increasing L/D	Increased	Decreased	Decreased
Increasing A_s/A_p	Increased	Increased	Increased
Increasing A_8/A_5	Increased	Decreased	Decreased

Results and Discussion

Flowfield Overview

Color contours of static pressure and Mach number of the RBCC internal flowpath for two configurations are shown in Figs. 3 and 4, respectively.The freestream zones downstream of the nozzle were omitted from Figs. 3 and 4. The rocket engine plume is clearly visible on the horizontal centerline. The Mach number contours indicate that the flow is entirely subsonic as it enters the diffuser section of the duct. The average Mach number at the nozzle exit was approximately 0.40. The pressure contours of the $A_s/A_p = 4.55$ case indicates that the primary flow attached to the mixture wall sooner and incurred significantly stronger shocks than the $A_s/A_p = 15.66$ configuration. The shocks were caused by the primary flow's interaction with the secondary flow and the mixer wall.

To compare the effect of duct aspect ratio on the RBCC internal flowpath, three configurations with $L/D = 7$, 14, and 21 were simulated. The increasing length of the inlet section reduces the inlet

Table 4 Figures of merit results for inlet/ejector trade study

Case	L/D	As/Ap	$A8/A5$	Bypass ratio	Ejector compression ratio	Mixer thrust efficiency	Desirability $D1$	Desirability $D2$	Desirability $D3$	Objective function, D
1	7	4.55	1.5	1.749	1.158	0.352	0.312	0.158	0.529	3.370
2	7	4.55	2	2.211	1.119	0.550	0.428	0.119	0.707	3.030
3	7	4.55	2.5	2.368	1.190	0.393	0.467	0.190	0.571	2.703
4	7	7.33	1.5	2.523	1.239	0.360	0.506	0.239	0.538	2.487
5	7	7.33	2	3.092	1.162	0.545	0.648	0.162	0.704	2.382
6	7	7.33	2.5	3.399	1.253	0.425	0.725	0.253	0.601	2.087
7	7	15.66	1.5	4.050	1.310	1.100	0.888	0.310	1.000	1.538
8	7	15.66	2	5.449	1.235	0.628	1.237	0.235	0.766	1.650
9	7	15.66	2.5	5.888	1.321	0.720	1.347	0.321	0.830	1.407
10	14	4.55	1.5	1.670	1.152	0.394	0.293	0.152	0.571	3.400
11	14	4.55	2	1.900	1.096	0.318	0.350	0.096	0.492	3.925
12	14	4.55	2.5	1.926	1.132	0.323	0.357	0.132	0.498	3.493
13	14	7.33	1.5	3.827	1.224	0.432	0.832	0.224	0.608	2.066
14	14	7.33	2	4.116	1.149	0.378	0.904	0.149	0.556	2.374
15	14	7.33	2.5	4.495	1.184	0.351	0.999	0.184	0.528	2.176
16	14	15.66	1.5	3.758	1.308	0.761	0.814	0.308	0.857	1.670
17	14	15.66	2	4.643	1.272	0.917	1.036	0.272	0.953	1.550
18	14	15.66	2.5	4.946	1.250	1.269	1.111	0.250	1.000	1.532
19	21	4.55	1.5	1.728	1.137	0.240	0.307	0.137	0.395	3.915
20	21	4.55	2	2.114	1.144	0.321	0.403	0.144	0.496	3.265
21	21	4.55	2.5	2.250	1.136	0.268	0.438	0.136	0.432	3.393
22	21	7.33	1.5	2.398	1.226	0.987	0.475	0.226	0.993	2.110
23	21	7.33	2	3.691	1.206	0.512	0.798	0.206	0.677	2.081
24	21	7.33	2.5	3.870	1.185	0.429	0.842	0.185	0.604	2.197
25	21	15.66	1.5	3.841	1.294	2.712	0.835	0.294	1.000	1.596
26	21	15.66	2	5.933	1.295	0.761	1.358	0.295	0.857	1.427
27	21	15.66	2.5	6.857	1.277	0.470	1.589	0.277	0.641	1.524

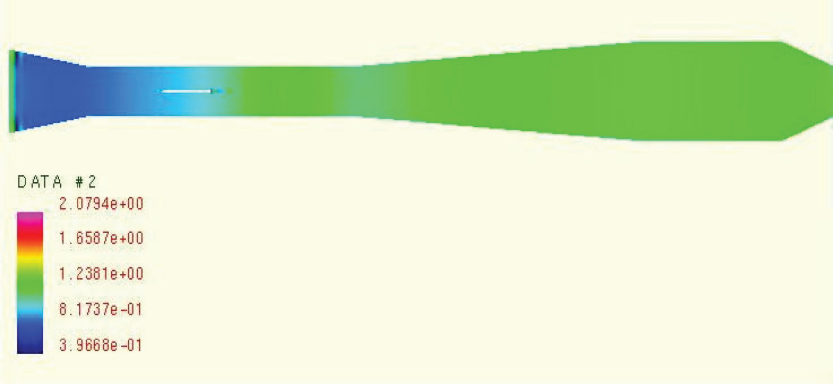

Fig. 4 Static pressure contour of RBCC engine internal flowpath for configuration $L/D = 7$, $A_s/A_p = 15.66$, and $A_8/A_5 = 2.0$ (case 8).

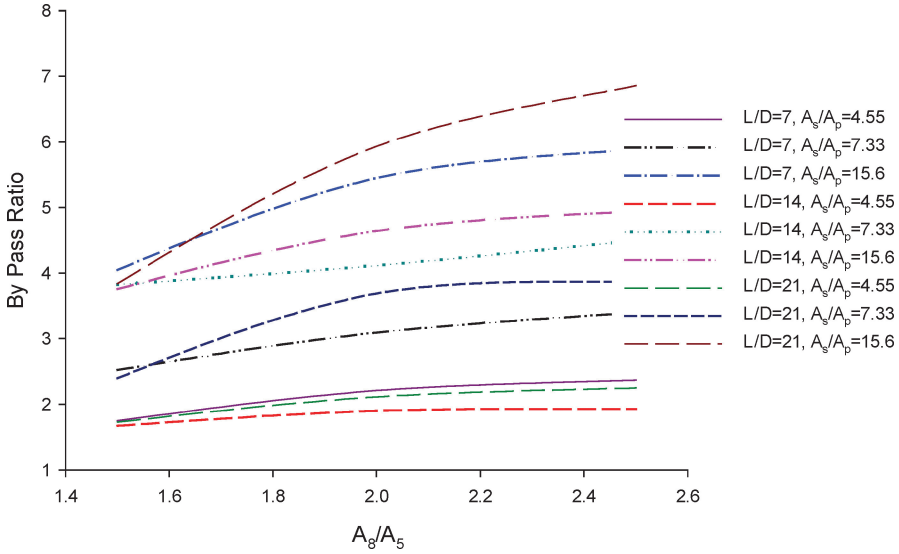

Fig. 5 Bypass ratio analysis.

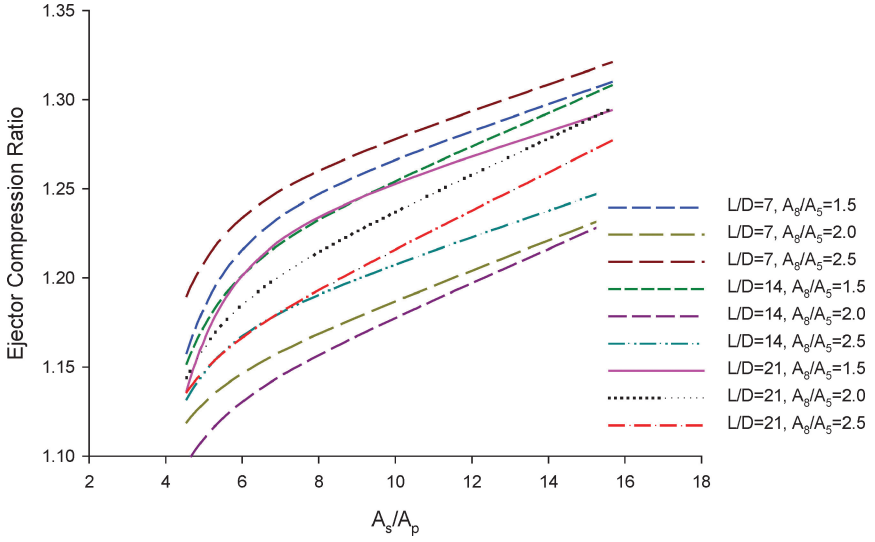

Fig. 6 ECR comparison.

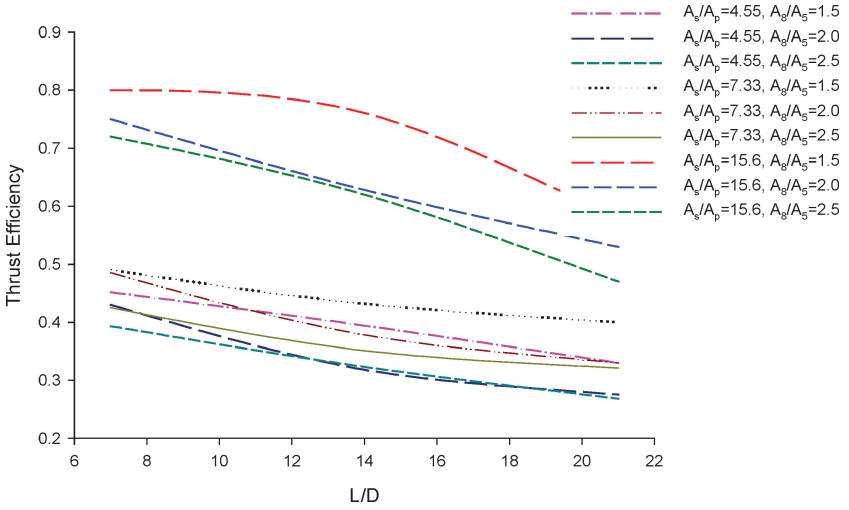

Fig. 7 Mixture thrust efficiency.

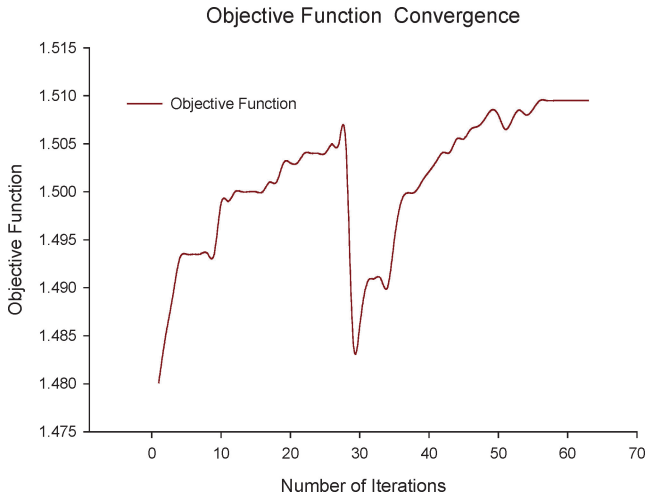

Fig. 8 Objective function convergence history.

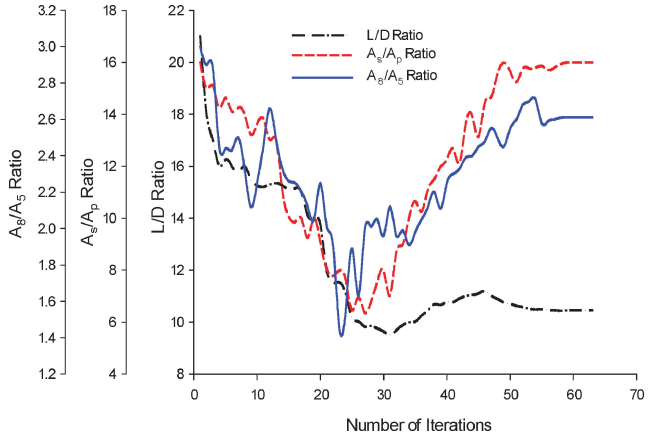

Fig. 9 Design variable convergence history.

angle, which increases the pressure recovery. Again, the additional length allows for another expansion and compression to occur in the mixer. The effect of design variables on bypass ratio, ECR, and thrust efficiency are shown in Figs. 5, 6, and 7, respectively, and the overall trend is summarized in Table 3.

Optimization Results

The CFD data of 27 cases were used to generate a response surface shown in Table 4. This response surface was used for training the NN, and later it was used for objective function evaluation. A spreadsheet was used to evaluate the individual and total desirability/objective function. After 63 iterations, the system level converged to the optimum value. Figure 8 shows a convergence history of the objective function. The value of objective function, at iteration number 30, jumps from one solution domain to another as it tries to reduce the interdisciplinary discrepancies. This phenomenon depends on the choice of the starting values of the design variables. Figure 9 shows the system level convergence of the design variables. Figure 9 shows that the values of each of the three design variables decreases to a minimum before increasing to an optimal value. The trend is opposite to the trend of the history of the objective function. The trend depends on the choice of the initial values of the design variables during optimization.

Conclusions

For the range of A_s/A_p studied, the smallest primary thruster ($A_s/A_p = 15.66$), pumped the most secondary flow. The $A_s/A_p = 15.66$ configuration clearly had the highest bypass ratio and best mixture thrust efficiency. Both L/D and A_8/A_5 had less dramatic, yet significant effects on bypass ratio. For this configuration, the rocket exit size was the smallest (0.762 cm). Again, the mixing results primarily from the turbulent and viscous shear forces in steady flow ejectors. Increasing the interfacial shear area between the primary and secondary flows will increase the mixing action in terms of required length. From this study, it is noticeable that smaller primary rockets have proven effective in reducing the mixing length, which agrees with the conceptual design of an RBCC engine.

Acknowledgment

This work has been supported by NASA Marshall Space Flight Center under Grant NAG8-1644.

References

[1]Escher, W. J. D., and Flornes, B. J., "A Study of Composite Propulsion Systems For Advanced Launch Vehicle Application," Contract NAS7-377, Marquardt Corp., Van Nuys, CA, 1966, Vol. 1–7.

[2]Steffen, C. J., Smith, T. D., Yungster, S., and Keller, D. J., "Rocket Based Combined Cycle Nozzle Analysis Using NPARC," AIAA Paper 98-0954, Jan. 1998.

[3]Chen, Y. S., and Liu, J., "User's Input and Data Guide-FDNS CFD Code, Version 5.0," Engineering Science, Inc., Huntsville, AL, June 1999.

[4]Ruf, J. H., "Benchmark of FDNS CFD Code For Direct Concept RBCC Test Data," AIAA Paper 2000-3726, July 2000.

[5]Wang, T. S., McConnaughey, P., Warsi, S., and Chen, Y. S., "Computational Pollutant Environment Assessment from Propulsion System Testing," *Journal of Spacecraft and Rockets*, Vol. 33, No. 3, 1996, pp. 386–392.

[6]Liou, T., Chen, L., and Wu, Y., "Effects of Momentum Ratio on Turbulent Nonreacting and Reacting Flows in a Ducted Rocket Combustor," *International Journal of Heat and Mass Transfer*, Vol. 36, No. 10, 1993, pp. 2589–2599.

[7]Gordon, S., and McBride, B. J., "Computer Program for Calculation of Complex Chemical Equilibrium Compositions and Applications," NASA Reference Publ. 1311, Oct. 1994.

[8]Sparks, D. W., and Maghami, P. G., "Neural Networks for Rapid Modeling and Analysis," AIAA Paper 98-1779, April 1998.

[9]Shyy, W., Tucker, K. P., and Vaidynathan, R., "Response Surface and Neural Network Techniques for Rocket Engine Injector Optimization," *Journal of Propulsion and Power*, Vol. 17, No. 2, 2001, pp. 391–401.

[10]Gill, P. E., Murray, W., Saunders, M. A., and Wright, M. H., "User's Guide for NPSOL (Version 4.0) - A Fortran Package for Nonlinear Programming," System Optimization Lab., Technical Rept. SOL 86-2, Stanford Univ., Palo Alto, CA, Jan. 1986.

[11]Eldred, C., Powdl, R., and Stanley, D., "Single Stage Rocket Options for Future Launch Vehicles," AIAA Paper 93-4162, Sept. 1993.